Available online at www.derpharmachemica.com

ISSN 0975-413X
CODEN (USA): PCHHAX

Der Pharma Chemica, 2016, 8(2):507-526
(http://derpharmachemica.com/archive.html)

A theoretical approach to the cytotoxicity of a series of β-carboline-dithiocarbamate derivatives against prostatic cancer (DU-145), breast cancer (MCF-7), human lung adenocarcinoma (A549) and cervical cancer (HeLa) cell lines

Juan S. Gómez-Jeria* and Sebastián Abarca-Martínez

Quantum Pharmacology Unit, Department of Chemistry, Faculty of Sciences, University of Chile. Las Palmeras 3425, Santiago, Chile

---

ABSTRACT

Here we present the results of a study relating molecular/electronic structure with cytotoxicity for a series of β-carboline-dithiocarbamate derivatives against four tumoral cell lines. The electronic structure of all systems was calculated at the B3LYP/6-31G(d,p) level with full geometry optimization. Statistically significant results were obtained for all tumoral cell lines. The analysis of the proposed pharmacophores allows identifying several atoms that can be used as targets for substitution and control of cytotoxicity.

Keywords: β-carboline-dithiocarbamate derivatives, β-carboline, QSAR, DFT, KPG model, DU-145, MCF-7, A549, HeLa, cytotoxicity, tumor cells.

INTRODUCTION

In general terms, cytotoxicity is the capacity of being toxic to cells. Cells exposed to a cytotoxic compound may suffer necrosis (they lose membrane integrity and die quickly as a consequence of cell lysis), they can halt growing and dividing or they can trigger a genetic program leading to cell death (apoptosis). Chemotherapy frequently depends on the ability of cytotoxic agents to kill or harm tumor cells. Throughout the previous years an intensive research has been carried out on the antitumor/cytotoxic/proapoptotic properties of numerous molecular systems on a variety of cancer cell lines [1-29].

In this paper we present the results of an analysis between the electronic and conformational properties of a series of β-carboline-dithiocarbamate derivatives and their cytotoxic activity against four tumoral cell lines. Besides the knowledge of the electronic foundations of cytotoxicity in this series, the resulting reactivity indices are being incorporated into a large database for further numerical analysis.

MATERIALS AND METHODS

The method [30].
Since the formal model employed here has been presented in numerous papers [31-39], we shall present here only its key lines of development and discuss below only the results obtained here. Starting from the statistical-mechanical

definition of the equilibrium constant, an expression linking any biological activity with several local atomic reactivity indices and orientational parameters was established. This model, called the Klopman-Peradejordi-Gómez model (KPG), is the only member of the class of formal models. Its application to quite a lot of diverse molecules and receptors gave very good results (see [39-55] and references therein). Its extension to all types of biological activities was very successful (see [54, 56-69] and references therein).

Selection of molecules and biological activities.

The selected molecules are a group of β-carboline-dithiocarbamate derivatives selected from a recent study [70]. The reported activities selected for this study are the cytotoxicities against prostatic cancer (DU-145), breast cancer (MCF-7), human lung adenocarcinoma (A549) and cervical cancer (HeLa) cell lines. Cytotoxicity was reported as the 50% inhibitory concentration after 48 h of drug treatment (IC_{50}, MTT assay). The general formula of molecules is shown in Fig. 1 and Table 1. The experimental cytotoxicities are displayed in Table 2.

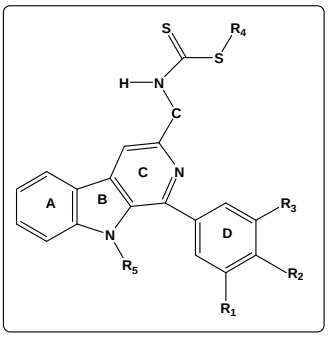

Figure 1. General formulas of β-carboline-dithiocarbamate derivatives

Table 1. β-carboline-dithiocarbamate derivatives

Mol.	R_1	R_2	R_3	R_4	R_5
1	OMe	OMe	OMe	Me	H
2	OMe	OMe	OMe	$CH_2CH(CH_2)$	H
3	OMe	OMe	OMe	$CH_2(C_6H_5)$	H
4	H	OMe	H	Me	H
5	H	OMe	H	$CH_2CH(CH_2)$	H
6	H	OMe	H	$CH_2(C_6H_5)$	H
7	H	CF_3	H	Me	H
8	H	CF_3	H	$CH_2CH(CH_2)$	H
9	H	CF_3	H	$CH_2(C_6H_5)$	H
10	H	F	H	Me	H
11	H	F	H	$CH_2CH(CH_2)$	H
12	H	F	H	$CH_2(C_6H_5)$	H
13	OMe	OMe	OMe	Me	Me
14	OMe	OMe	OMe	$CH_2CH(CH_2)$	Me
15	OMe	OMe	OMe	$CH_2(C_6H_5)$	Me
16	H	OMe	H	Me	Me
17	H	OMe	H	$CH_2CH(CH_2)$	Me
18	H	OMe	H	$CH_2(C_6H_5)$	Me
19	H	CF_3	H	Me	Me
20	H	CF_3	H	$CH_2CH(CH_2)$	Me
21	H	CF_3	H	$CH_2(C_6H_5)$	Me
22	H	F	H	Me	Me
23	H	F	H	$CH_2CH(CH_2)$	Me
24	H	F	H	$CH_2(C_6H_5)$	Me

Table 2. Cytotoxicity of the β-carboline-dithiocarbamate derivatives

Mol.	log(IC_{50}) A549	log(IC_{50}) MCF-7	log(IC_{50}) DU-145	log(IC_{50}) HeLa
1	0.91	0.95	0.75	1.05
2	1.11	1.20	1.14	1.37
3	1.44	1.41	1.24	1.16
4	0.90	0.93	0.06	0.89
5	1.71	1.59	1.67	1.77
6	1.25	1.00	1.14	1.38
7	1.23	1.20	0.98	1.10
8	1.27	1.04	0.89	1.03
9	0.97	1.09	0.77	0.60
10	0.64	0.39	0.13	0.54
11	1.22	0.82	0.60	0.65
12	1.60	0.87	0.57	0.58
13	1.10	1.18	0.79	1.23
14	1.26	1.31	1.29	1.30
15	1.15	1.14	1.03	1.09
16	0.71	0.18	0.15	0.41
17	1.00	0.51	0.40	0.92
18	0.96	0.53	0.84	1.14
19	0.55	0.04	-0.10	0.17
20	0.63	0.68	0.30	0.67
21	0.71	0.63	0.32	0.68
22	0.75	0.27	0.16	0.38
23	0.78	0.48	0.46	0.41
24	0.83	0.44	0.68	0.50

Calculations.

The electronic structure of all molecules was calculated within the Density Functional Theory (DFT) at the B3LYP/6-31g(d,p) level with full geometry optimization. The Gaussian suite of programs was used [71]. All the information needed to calculate numerical values for the local atomic reactivity indices was obtained from the Gaussian results with the D-Cent-QSAR software [72]. All the electron populations smaller than or equal to 0.01 e were considered as zero [31]. Negative electron populations coming from Mulliken Population Analysis were corrected as usual [73]. As the resolution of the system of linear equations is not possible because we have not sufficient molecules, we employed Linear Multiple Regression Analysis (LMRA) techniques to find the best solution. For each case, a matrix containing the dependent variable (the biological activity of each case) and the local atomic reactivity indices of all atoms of the common skeleton as independent variables was built. The Statistica software was used for LMRA [74].

We worked within the *common skeleton approximation* stating that there is a collection of atoms, common to all molecules analyzed, that accounts for virtually all the biological activity. The action of the substituents consist on the modification of the electronic structure of the common skeleton and the influence on the right alignment of the drug through the orientational parameters. It is hypothesized that diverse parts or this common skeleton accounts for almost all the interactions leading to the expression of a given biological activity. The common skeleton for the dithiocarbamate linked β-carboline derivatives is shown in Fig. 2.

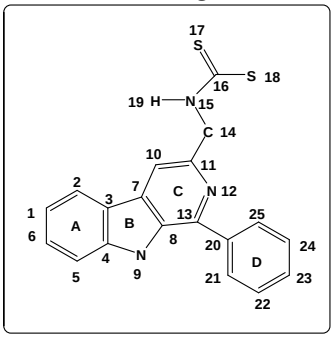

Figure 2. Common skeleton of β-carboline-dithiocarbamate derivatives

RESULTS

Cytotoxicity against the A549 cell line.
The best equation obtained was:

$$\log(IC_{50}) = -23.95 - 205.40Q_5 + 2.43F_{13}(HOMO)^* - 1.41F_{15}(HOMO-2)^* + \\ +0.007S_1^N(LUMO+1)^* - 0.03S_{15}^N(LUMO+1)^* - 4.93F_{14}(LUMO+1)^* \quad (1)$$

with n=24, R=0.95, R^2=0.90, adj-R^2=0.86, F(6,17)=25.50 (p<0.0001) and SD=0.11. No outliers were detected and no residuals fall outside the ±2σ limits. Here, Q_5 is the net charge of atom 5, $F_{13}(HOMO)^*$ is the electron population (Fukui index) of the highest occupied (local) MO localized on atom 13, $F_{15}(HOMO-2)^*$ is the Fukui index of the third highest occupied MO localized on atom 15, $S_1^N(LUMO+1)^*$ is the nucleophilic superdelocalizability of the second lowest empty MO localized on atom 1, $S_{15}^N(LUMO+1)^*$ is the nucleophilic superdelocalizability of the second lowest vacant MO localized on atom 15 and $F_{14}(LUMO+1)^*$ is the Fukui index of the second lowest vacant MO localized on atom 14. Tables 3 and 4 show the beta coefficients, the results of the t-test for significance of coefficients and the matrix of squared correlation coefficients for the variables of Eq. 1. There are no significant internal correlations between independent variables (Table 4). Figure 3 displays the plot of observed *vs*. calculated log(IC_{50}).

Table 3. Beta coefficients and t-test for significance of coefficients in Eq. 1

	Beta	t(17)	p-level
Q_5	-0.79	-9.50	<0.000001
$F_{13}(HOMO)^*$	0.32	3.67	<0.002
$F_{15}(HOMO-2)^*$	-0.41	-5.04	<0.0001
$S_1^N(LUMO+1)^*$	0.43	4.67	<0.0002
$S_{15}^N(LUMO+1)^*$	-0.36	-4.41	<0.0004
$F_{14}(LUMO+1)^*$	-0.25	-2.97	<0.009

Table 4. Matrix of squared correlation coefficients for the variables in Eq. 1

	Q_5	$F_{13}(HOMO)^*$	$F_{15}(HOMO-2)^*$	$S_1^N(LUMO+1)^*$	$S_{15}^N(LUMO+1)^*$
$F_{13}(HOMO)^*$	0.006	1			
$F_{15}(HOMO-2)^*$	0.03	0.008	1		
$S_1^N(LUMO+1)^*$	0.002	0.19	0.01	1	
$S_{15}^N(LUMO+1)^*$	0.0009	0.0001	0.008	0.08	1
$F_{14}(LUMO+1)^*$	0.11	0.02	0.04	0.0004	0.0009

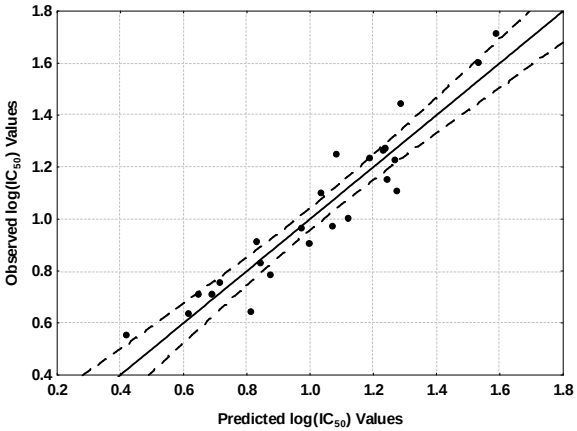

Figure 3. Plot of predicted *vs*. observed log(IC_{50}) values (Eq. 1). Dashed lines denote the 95% confidence interval

The associated statistical parameters of Eq. 1 indicate that this equation is statistically significant and that the variation of the numerical values of a group of six local atomic reactivity indices of atoms of the common skeleton explains about 86% of the variation of log(IC_{50}) in this group of β-carboline-dithiocarbamate derivatives. Figure 3, spanning about 1.6 orders of magnitude, shows that there is a good correlation of observed *versus* calculated values and that almost all points are inside the 95% confidence interval. This can be considered as an indirect evidence that the common skeleton hypothesis works relatively well for this set of molecules.

A noteworthy point to comment on is the following. When a local atomic reactivity index of an inner occupied MO (i.e., HOMO-1 and/or HOMO-2) or of a higher vacant MO (LUMO+1 and/or LUMO+2) appears in any equation, this means that the remaining of the upper occupied MOs (for example, if HOMO-2 appears, upper means HOMO-1 and HOMO) or the remaining of the empty MOs (for example, if LUMO+1 appears, lower means the LUMO) contribute to the interaction. Their absence in the equation only means that the variation of their numerical values does not account for the variation of the numerical value of the biological property.

Cytotoxicity against the MCF-7 cell line.

The best equation obtained was:

$$\log(IC_{50}) = -0.44 - 9.95Q_{21} - 2.46F_5(LUMO+2)* + \\ +4.03F_1(HOMO-1)* + 1.95S_7^E(HOMO-1)* + 0.19S_{12}^E(HOMO-1)* \quad (2)$$

with n=23, R=0.97, R^2=0.93, adj-R^2=0.91, F(5,17)=48.03 (p<0.00001) and SD=0.12. No outliers were detected and no residuals fall outside the ±2σ limits. Here, Q_{21} is the net charge of atom 21, $F_5(LUMO+2)*$ is the Fukui index of the third lowest vacant MO localized on atom 5, $F_1(HOMO-1)*$ is the Fukui index of the second highest occupied MO localized on atom 1, $S_7^E(HOMO-1)*$ is the total atomic electrophilic superdelocalizability of the second highest occupied MO localized on atom 7 and $S_{12}^E(HOMO-1)*$ is the total atomic electrophilic superdelocalizability of the second highest occupied MO localized on atom 12. Tables 5 and 6 show the beta coefficients, the results of the t-test for significance of coefficients and the matrix of squared correlation coefficients for the variables of Eq. 2. There is a significant internal correlation between a couple of independent variables ($S_7^E(HOMO-1)*$ and $F_1(HOMO-1)*$, see Table 6). This indicates that we must take with caution the values of the associated statistical parameters of Eq. 2. Figure 4 displays the plot of observed *vs.* calculated log(IC_{50}).

Table 5. Beta coefficients and t-test for significance of coefficients in Eq. 2

	Beta	t(17)	p-level
Q_{21}	-0.82	-10.45	<0.000001
$F_5(LUMO+2)^*$	-0.37	-5.03	<0.0001
$F_1(HOMO-1)^*$	0.59	6.41	<0.000006
$S_7^E(HOMO-1)^*$	0.38	4.15	<0.0007
$S_{12}^E(HOMO-1)^*$	0.18	2.44	<0.03

Table 6. Matrix of squared correlation coefficients for the variables in Eq. 2

	Q_{21}	$F_5(LUMO+2)^*$	$F_1(HOMO-1)^*$	$S_7^E(HOMO-1)^*$
$F_5(LUMO+2)^*$	0.10	1		
$F_1(HOMO-1)^*$	0.17	0.22	1	
$S_7^E(HOMO-1)^*$	0.26	0.16	0.46	1
$S_{12}^E(HOMO-1)^*$	0.22	0.01	0.18	0.12

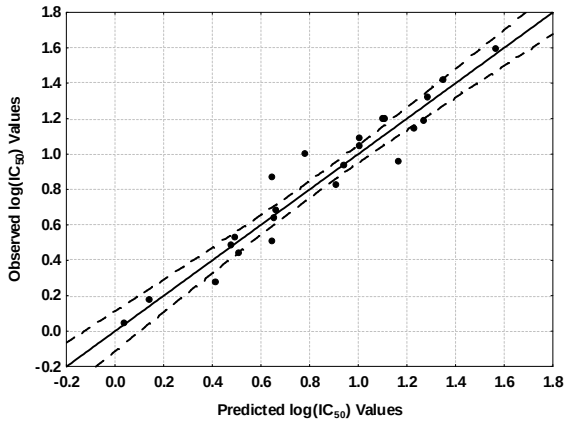

Figure 4. Plot of predicted *vs*. observed log(IC_{50}) values (Eq. 2). Dashed lines denote the 95% confidence interval

The associated statistical parameters of Eq. 2 indicate that this equation is statistically significant and that the variation of the numerical values of a group of five local atomic reactivity indices of atoms of the common skeleton explains about 91% of the variation of log(IC_{50}) in this group of β-carboline-dithiocarbamate derivatives. Figure 4, spanning about 2 orders of magnitude, shows that there is a good correlation of observed *versus* calculated values and that almost all points are inside the 95% confidence interval. This can be considered as an indirect evidence that the common skeleton hypothesis works relatively well for this set of molecules.

Cytotoxicity against the DU-145 cell line.

The best equation obtained was:

$$\log(IC_{50}) = 1.22 - 0.84F_{25}(LUMO+2)^* - 2.72F_{17}(LUMO+2)^* + 2.70F_1(LUMO+1)^* + \\ +0.11S_{23}^N(LUMO+1)^* + 0.59S_{22}^E(HOMO-1)^* - 0.005S_{16}^N(LUMO+2)^* \quad (3)$$

with n=24, R=0.96, R^2=0.92, adj-R^2=0.89, F(6,17)=30.77 (p<0.00001) and SD=0.15. No outliers were detected and no residuals fall outside the ±2σ limits. Here, $F_{25}(LUMO+2)^*$ is the Fukui index of the third lowest vacant MO localized on atom 25, $F_{17}(LUMO+2)^*$ is the Fukui index of the third lowest vacant MO localized on atom 17, $F_1(LUMO+1)^*$ is the Fukui index of the second lowest vacant MO localized on atom 1, $S_{23}^N(LUMO+1)^*$ is the nucleophilic superdelocalizability of the second lowest vacant MO localized on atom 23, $S_{22}^E(HOMO-1)^*$ is the electrophilic superdelocalizability of the second highest occupied MO localized on atom 22 and $S_{16}^N(LUMO+2)^*$ is the nucleophilic superdelocalizability of the third lowest vacant MO localized on atom 16. Tables 7 and 8 show the beta coefficients, the results of the t-test for significance of coefficients and the matrix of squared correlation coefficients for the variables of Eq. 3. There is a significant internal correlation between a couple of independent variables ($S_{23}^N(LUMO+1)^*$ and $F_{25}(LUMO+2)^*$, see Table 8). This indicates that we must take with caution the values of the associated statistical parameters of Eq. 3. Figure 5 displays the plot of observed *vs.* calculated log(IC_{50}).

Table 7. Beta coefficients and t-test for significance of coefficients in Eq. 3

	Beta	t(17)	p-level
$F_{25}(LUMO+2)^*$	-0.39	-4.09	<0.0008
$F_{17}(LUMO+2)^*$	-0.29	-3.75	<0.002
$F_1(LUMO+1)^*$	0.63	7.25	<0.000001
$S_{23}^N(LUMO+1)^*$	0.44	4.19	<0.0006
$S_{22}^E(HOMO-1)^*$	0.29	3.46	<0.003
$S_{16}^N(LUMO+2)^*$	-0.21	-2.83	<0.01

Table 8. Matrix of squared correlation coefficients for the variables in Eq. 3

	$F_{25}(LUMO+2)^*$	$F_{17}(LUMO+2)^*$	$F_1(LUMO+1)^*$	$S_{23}^N(LUMO+1)^*$	$S_{22}^E(HOMO-1)^*$
$F_{17}(LUMO+2)^*$	0.0004	1			
$F_1(LUMO+1)^*$	0.02	0.01	1		
$S_{23}^N(LUMO+1)^*$	0.41	0.03	0.14	1	
$S_{22}^E(HOMO-1)^*$	0.06	0.05	0.16	0.10	1
$S_{16}^N(LUMO+2)^*$	0.01	0.006	0.0001	0.05	0.03

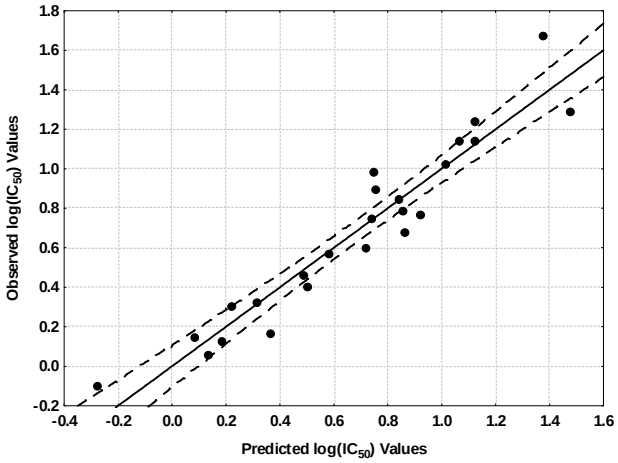

Figure 5. Plot of predicted *vs*. observed log(IC_{50}) values (Eq. 3). Dashed lines denote the 95% confidence interval

The associated statistical parameters of Eq. 3 indicate that this equation is statistically significant and that the variation of the numerical values of a group of six local atomic reactivity indices of atoms of the common skeleton explains about 89% of the variation of log(IC_{50}) in this group of β-carboline-dithiocarbamate derivatives. Figure 5, spanning about 2 orders of magnitude, shows that there is a good correlation of observed *versus* calculated values and that almost all points are inside the 95% confidence interval. This can be considered as an indirect evidence that the common skeleton hypothesis works relatively well for this set of molecules.

Cytotoxicity against the HeLa cell line.

The best equation obtained was:

$$\log(IC_{50}) = 0.78 - 1.77S_6^E(HOMO-1)^* - 0.04S_{17}^N(LUMO+1)^* - \\ -2.68F_{15}(LUMO+1)^* + 0.55S_{22}^E(HOMO-1)^* - 2.13F_{12}(LUMO+2)^* \quad (4)$$

with n=24, R=0.95, R^2=0.91, adj-R^2=0.88, F(5,18)=35.04 (p<0.00001) and SD=0.14. No outliers were detected and no residuals fall outside the ±2σ limits. Here, $F_{15}(LUMO+1)^*$ is the Fukui index of the second lowest vacant MO localized on atom 15, $F_{12}(LUMO+2)^*$ is the Fukui index of the third lowest vacant MO localized on atom 12, $S_6^E(HOMO-1)^*$ is the electrophilic superdelocalizability of the second highest occupied MO localized on atom 6, $S_{22}^E(HOMO-1)^*$ is the electrophilic superdelocalizability of the second highest occupied MO localized on atom 22 and $S_{17}^N(LUMO+1)^*$ is the nucleophilic superdelocalizability of the second lowest vacant MO localized on atom 17. Tables 9 and 10 show the beta coefficients, the results of the t-test for significance of coefficients and the matrix of squared correlation coefficients for the variables of Eq. 4. There are no significant internal correlations between independent variables (Table 10). Figure 6 displays the plot of observed *vs*. calculated log(IC_{50}).

Table 9. Beta coefficients and t-test for significance of coefficients in Eq. 4

	Beta	t(18)	p-level
$S_6^E(HOMO-1)^*$	-0.80	-10.15	<0.000000
$S_{17}^N(LUMO+1)^*$	-0.58	-6.63	<0.000003
$F_{15}(LUMO+1)^*$	-0.49	-5.72	<0.00002
$S_{22}^E(HOMO-1)^*$	0.31	3.94	<0.001
$F_{12}(LUMO+2)^*$	-0.21	-2.67	<0.02

Table 10. Matrix of squared correlation coefficients for the variables in Eq. 4

	$S_6^E(HOMO-1)^*$	$S_{17}^N(LUMO+1)^*$	$F_{15}(LUMO+1)^*$	$S_{22}^E(HOMO-1)^*$
$S_{17}^N(LUMO+1)^*$	0.14	1	0	0
$F_{15}(LUMO+1)^*$	0.07	0.26	1	0
$S_{22}^E(HOMO-1)^*$	0.004	0.01	0.04	1
$F_{12}(LUMO+2)^*$	0.0001	0.01	0.01	0.09

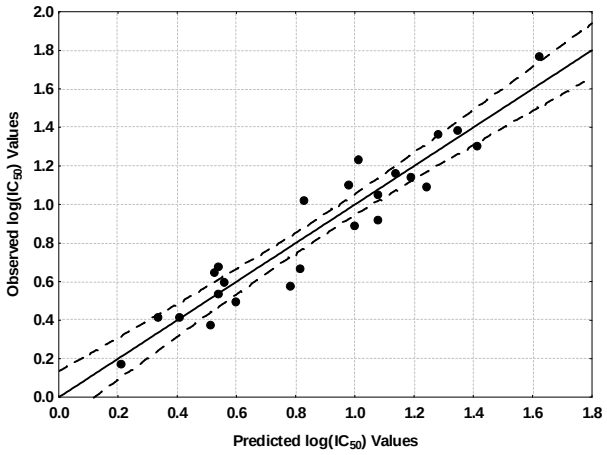

Figure 6. Plot of predicted *vs*. observed log(IC_{50}) values (Eq. 4). Dashed lines denote the 95% confidence interval

The associated statistical parameters of Eq. 4 indicate that this equation is statistically significant and that the variation of the numerical values of a group of five local atomic reactivity indices of atoms of the common skeleton explains about 88% of the variation of log(IC_{50}) in this group of β-carboline-dithiocarbamate derivatives. Figure 6, spanning about 1.8 orders of magnitude, shows that there is a good correlation of observed *versus* calculated values and that almost all points are inside the 95% confidence interval. This can be considered as an indirect evidence that the common skeleton hypothesis works relatively well for this set of molecules.

Local Molecular Orbitals.

Tables 11-14 show the local MO structure of atoms appearing in Eqs. 1-4 (see Fig. 2). Nomenclature: Molecule (HOMO) / (HOMO-2)* (HOMO-1)* (HOMO)* - (LUMO)* (LUMO+1)* (LUMO+2)*.

Table 11. Local molecular orbital structure of atoms 1, 5, 6 and 7

Mol.	Atom 1 (C)	Atom 5 (C)	Atom 6 (C)	Atom 7 (C)
1 (119)	115π116π119π-121π122π123π	115π116π119π-120π121π122π	108π109π114π-120π122π123π	115π116π119π-120π122π123π
2 (126)	123π124π126π-128π129π131π	123π124π126π-127π128π129π	114π115π121π-127π129π130π	122π123π126π-127π129π131π
3 (139)	135π136π139π-142π143π145π	135π136π139π-140π141π142π	126π127π134π-140π142π143π	135π136π139π-140π142π143π
4 (103)	100π102π103π-106π108π109π	100π102π103π-104π106π107π	92π 94π 99π-104π106π107π	100π102π103π-104π106π108π
5 (110)	106π107π110π-113π116π117π	106π107π110π-111π113π114π	98π100π106π-111π113π115π	106π107π110π-111π113π116π
6 (123)	120π122π123π-125π126π127π	120π122π123π-124π125π126π	110π112π119π-124π126π127π	120π122π123π-124π126π127π
7 (111)	108π109π110π-113π116π117π	108π109π110π-112π113π115π	102π103π108π-112π113π115π	108π109π110π-112π113π116π
8 (118)	115π116π117π-120π123π124π	115π116π117π-119π120π122π	108π109π115π-119π120π122π	115π116π117π-119π120π125π
9 (131)	128π129π130π-133π137π139π	128π129π130π-132π133π135π	120π121π128π-132π133π135π	128π129π130π-132π133π137π
10 (99)	96π97π98π-101π103π104π	96π97π98π-100π101π103π	90π91π96π-100π101π103π	96π97π98π-100π101π104π
11 (106)	104π105π106π-108π110π112π	104π105π106π-107π108π110π	96π 97π103π-107π108π110π	103π104π105π-107π108π112π
12 (119)	116π117π118π-121π124π126π	116π117π118π-120π121π124π	108π109π116π-120π121π124π	116π117π118π-120π121π126π
13 (123)	119π120π123π-126π127π128π	119π120π123π-124π126π 127π	112π113π118π-124π126π127π	119π120π123π-124π126π127π
14 (130)	126π127π130π-133π135π136π	126π127π130π-131π133π134π	118π119π125π-131π133π134π	126π127π130π-131π133π135π
15 (143)	140π141π143π-145π147π149π	140π141π143π-144π145π146π	130π131π138π-144π147π149π	139π140π143π-144π145π147π
16 (107)	104π106π107π-110π112π113π	104π106π107π-108π110π112π	98π99π103π-108π110π112π	103π104π107π-108π110π112π
17 (114)	110π111π114π-117π120π121π	110π111π114π-115π117π119π	101π104π110π-115π117π119π	110π111π114π-115π117π120π
18 (127)	124π126π127π-130π131π134π	124π126π127π-128π130π131π	116π117π123π-128π130π131π	124π126π127π-128π130π131π
19 (115)	112π113π114π-117π120π121π	112π113π114π-116π117π121π	106π107π112π-116π117π120π	112π113π114π-116π117π120π
20 (122)	120π121π122π-124π127π128π	120π121π122π-123π124π128π	112π113π119π-123π124π127π	119π120π121π-123π124π129π
21 (135)	132π133π134π-137π141π143π	132π133π134π-136π137π141π	124π125π132π-136π137π140π	132π133π134π-136π137π141π
22 (103)	101π102π103π-105π108π109π	101π102π103π-104π105π106π	94π95π100π-104π105π106π	101π102π103π-104π105π108π
23 (110)	108π109π110π-112π113π116π	108π109π110π-111π112π113π	100π101π107π-111π112π113π	108π109π110π-111π112π113π
24 (123)	121π122π123π-125π127π130π	121π122π123π-124π125π126π	112π113π120π-124π125π127π	120π122π123π-124π125π127π

Table 12. Local molecular orbital structure of atoms 12, 13, 14 and 15

Mol.	Atom 12 (N)	Atom 13 (C)	Atom 14 (C)	Atom 15 (N)
1 (119)	114π116σ119π-120π122π123π	115π116π119π-120π121π122π	113σ117σ118σ-122σ123σ126σ	113π117π119π-121σ122π128σ
2 (126)	123σ124π126π-127π128π129π	123π124π126π-127π128π129π	119σ120σ125σ-129π130σ131σ	120π124π126π-128π129π131σ
3 (139)	134π136σ139π-140π142π145π	130σ135π139π-140π142π143π	130σ137σ138σ-142σ145σ148σ	133π137π139σ-141π142σ144π
4 (103)	100π102π103π-104π106π108π	100π102π103π-104π106π111π	98σ101σ102σ-106π108π110σ	101π102σ103σ-105π112σ134σ
5 (110)	107π108π110π-111π113π115π	107π109π110π-111π113π119π	103σ105σ109σ-112σ113π115π	108σ109σ110σ-112σ113σ118σ
6 (123)	119π120π122π-124π126π130π	120π122π123π-124π125π126π	114σ115σ122σ-126σ130π132σ	121π122σ123σ-125π126π129π
7 (111)	105σ106π108π-112π113π116π	106π109π110π-112π113π116π	107σ110σ111σ-116π117π118σ	109π110π111σ-114π120σ130σ
8 (118)	113π115π116π-119π120π123π	113π116π117π-119π120π123π	114σ117σ118σ-123π125σ127σ	116π117π118σ-121π127σ137σ
9 (131)	124π128π129π-132π133π137π	124π129π130π-132π133π137π	123σ130σ131σ-136σ137σ139π	129π130π131σ-134π137σ142σ
10 (99)	95π96π97π - 100π101π104π	97π98π99π-100π101π103π	94σ98σ99σ-101π104π106σ	97π98π99σ-102π108σ114σ
11 (106)	101π103π104π-107π108π111π	104π105π106π-107π108π110π	99σ105σ106σ-108π111π112σ	104π105π106σ-108π109π114σ
12 (119)	113π116π117π-120π121π126π	113π117π118π-120π121π124π	111σ118σ119σ-121π126π127π	117π118π119σ-122π126σ130σ
13 (123)	120σ121π123π-124π126π 127π	119π120π123π-124π125π126π	117σ121σ122σ-126π127π130σ	120π121π123π-125π126π132σ
14 (130)	127σ128π130π-131π133π134π	126π127π130π-131π133π135π	124σ128σ129σ-133π134σ136σ	128π129σ130π-132π136σ138σ
15 (143)	140σ141σ143π-144π145π147π	140π141π143π-144π145π147π	137σ141σ142σ-145π146σ147σ	140π141π143π-145π146π147π
16 (107)	104π106π107π-108π110π112π	104π106π107π-108π110π115π	102σ105σ106σ-110π112π114σ	105π106σ107σ-109π116σ123σ
17 (114)	110π111π114π-115π117π119π	108σ111π114π-115π117π120π	109σ112σ113σ-116σ117π119σ	112π113σ114σ-116π117π122σ
18 (127)	124π126π127π-128π130π134π	124π126π127π-128π130π131π	119σ125σ126σ-130π134π135π	125π126σ127σ-129π133π134σ
19 (115)	110σ112π114σ-116π117π120π	113π114π115π-116π117π120π	111σ114σ115σ-120π121π122σ	113π114π115σ-118π124σ137σ
20 (122)	117σ119π121σ-123π124π127π	120π121π122π-123π124π127π	118σ121σ122σ-127π128σ129σ	120π121π122σ-125π127σ131σ
21 (135)	127σ128σ132π-136π137π141π	128π133π134π-136π137π141π	127σ134σ135σ-140σ141σ143π	133π134π135σ-138π141σ146σ
22 (103)	99σ100π102π-104π105π108π	101π102π103π-104π105π108π	97σ98σ102σ-105σ106σ108π	101π102π103σ-105π106π112σ
23 (110)	105σ106σ107π-111π112π113π	108π109π110π-111π112π113π	103σ106σ109σ-113σ115σ116σ	108π109σ110σ-112π113π118σ
24 (123)	119σ120π122π-124π125π130π	121π122π123π-124π125π127π	118σ121σ122σ-125π126σ130π	121π122σ123σ-125π126π127σ

Table 13. Local molecular orbital structure of atoms 16, 17, 21 and 22

Mol.	Atom 16 (C)	Atom 17 (S)	Atom 21 (C)	Atom 22 (C)
1 (119)	113π117π118π-121π122π123π	117π118π119π-121lp122lp123lp	98σ100π101π-131π132π134π	98σ100π101π-129σ130σ132σ
2 (126)	120π124π125π-128π129π130π	124π125π126π-128lp129lp130π	96σ104σ107π-140σ144σ146π	91σ104σ107π-137σ138σ140σ
3 (139)	133π137π138σ-141π142π143σ	137π138π139π-141lp142lp143lp	115π117σ118σ-153σ154σ155σ	115π117σ118π-150σ152σ154σ
4 (103)	101π102π103π-105π108π110σ	101π102π103π-105lp108lp110π	88σ89σ90σ-113σ114σ116σ	87σ88σ89σ-113σ115σ116σ
5 (110)	105π108π109π-112π113π115π	108π109π110π-112lp113lp115π	94π95π96σ-121σ122σ124σ	92σ94π95π-121σ123σ124σ
6 (123)	121π122π123σ-125π126π127σ	121π122π123π-125lp126lp129lp	100σ102σ105σ-136π138π139σ	100σ102σ105σ-135σ137σ138π
7 (111)	109π110π111π-113π114π116π	109π110π111π-113lp114lp116lp	97σ 98σ 99σ-121σ122σ123σ	97σ 98σ 99π-121σ122σ123σ
8 (118)	116π117π118π-121π123π124σ	116π117π118π-121lp123lp124π	102σ104σ106σ-129σ130π131π	100π102σ104σ-129σ131π132σ
9 (131)	129π130π131σ-134π136π137σ	129π130π131π-134lp136π138lp	112π115σ116σ-143σ144π145π	94σ112π115σ-143σ145π147σ
10 (99)	97π98π99π-101π102π104π	97π98π99π-102lp104lp106π	85π87σ88σ-110σ111σ112σ	85π87σ88σ-109σ111σ113π
11 (106)	104π105π106π-108π109π111σ	104π105π106π-108lp109lp111π	91σ92σ94σ-118σ119σ120σ	90π91σ92σ-117σ119σ121π
12 (119)	117π118π119π-121π122π123σ	117π118π119π-122lp125lp126lp	98π100π103σ-132π133σ134σ	98π100π103σ-131σ133σ136π
13 (123)	119π121π122π-125π126π127σ	121π122π123π-125lp126lp127π	104σ105σ106σ-135π136σ137σ	104σ105σ106π-133σ134σ136σ
14 (130)	126π128π129π-132π134π138σ	128π129π130π-132lp134π136π	110π111σ112σ-144σ145σ147σ	110π111σ112π-141σ142σ144σ
15 (143)	139π141π142π-145π146σ147π	141π142π143π-145lp146lp147lp	122π123σ124π-158π159σ160σ	122π123σ124π-155σ156σ159σ
16 (107)	102π105π106π-109π110π112π	105π106π107π-109lp112lp113π	91σ92σ93π-117σ118σ119σ	91σ92σ93π-117σ118σ119σ
17 (114)	109π112π113π-116π117π119σ	112π113π114π-116lp117lp119π	96σ98σ99π-125σ127σ128σ	96σ98σ99π-125σ127σ128σ
18 (127)	122σ125π126π-129π130σ131σ	125π126π127π-129lp133lp134lp	104σ106σ109σ-139σ140σ141σ	104σ106σ109σ-139σ141σ143σ
19 (115)	113π114π115π-118π120π121π	113π114π115π-118lp121lp122π	99σ101σ103σ-125σ126σ127σ	99σ101σ103σ-125σ127σ128π
20 (122)	120π121π122π-125π127π128σ	120π121π122π-125lp127lp128π	106σ108σ109σ-133σ134σ135σ	106σ108σ109σ-133σ135σ136π
21 (135)	133π134π135π-138π140σ141σ	133π134π135π-138lp140π142lp	100π116σ119σ-147σ148σ149σ	100π116σ119σ-147σ149σ151π
22 (103)	101π102π103π-105π106π108π	101π102π103π-105lp106lp108lp	88σ89σ91π-114σ115σ116σ	88σ8991π-113σ115σ116σ
23 (110)	108π109π110π-112π113π115σ	108π109π110π-112lp113lp115π	93π95σ97π-123σ124σ125π	93π95σ97π-121σ123σ124σ
24 (123)	121π122π123π-125π126π127π	121π122π123π-125π126lp127lp	105σ107π109σ-137σ138σ139σ	103π107π109σ-135σ137σ138σ

Table 14. Local molecular orbital structure of atoms 23 and 25

Mol.	Atom 23 (C)	Atom 25 (C)
1 (119)	99σ100σ101σ-132σ137π138π	95σ99σ112π-131σ132σ133σ
2 (126)	103σ105σ107π-140σ146π157π	100σ105σ118σ-140σ142σ144σ
3 (139)	112σ114σ117σ-154σ155σ157σ	112σ114σ130σ-153σ154σ155σ
4 (103)	86σ87σ89σ-115σ116σ118σ	88σ96π97π-113σ114σ116σ
5 (110)	93σ94π95π-123σ124σ126σ	93σ102π103π-121σ122σ124σ
6 (123)	101σ103σ105σ-137σ138π139σ	104σ114π115π-135σ136π139σ
7 (111)	95π97σ99π-122σ123σ126σ	94π98σ105π-121σ122σ123σ
8 (118)	102σ103σ104σ-131π134σ139σ	103σ110π111π-129σ130π131π
9 (131)	112π113σ115σ-144π145π149σ	110σ113σ123π-143σ144π145π
10 (99)	81σ84σ87σ-111σ112σ113π	77σ84σ93π-109σ110σ111σ
11 (106)	89σ91σ92σ-119σ120σ121π	82σ89σ99π-117σ118σ119σ
12 (119)	99σ100π103σ-133σ135σ136π	91σ99σ111π-131σ132π133σ
13 (123)	103σ105σ106σ-136σ138σ140σ	120π121π123π-124π125π126π
14 (130)	108σ111σ112σ-144σ146σ148σ	127π128π130π-131π133π134π
15 (143)	121σ122π123σ-158π159σ160σ	141π142π143π-144π145π147π
16 (107)	90σ91σ93π-117σ118σ119σ	105π106π107π-108π110π111π
17 (114)	96σ97σ99π-125σ127σ128σ	111π112π114π-115π117π118π
18 (127)	106σ107σ109σ-139σ140σ141σ	125π126π127π-128π130π131π
19 (115)	99σ101σ103σ-125σ127σ128π	109π1101σ14π-116π117π119π
20 (122)	103σ106σ108σ-133σ135σ136π	116π117π121π-123π124π126π
21 (135)	116σ117σ119σ-147σ149σ151π	128π129π134π-136π137π139π
22 (103)	86σ88σ91π-115σ116σ117π	98π99π102π-104π105π106π
23 (110)	94σ95σ97π-123σ124σ125π	108π109π110π-111π112π113π
24 (123)	104σ105σ107π-137σ138σ139σ	119π122π123π-124π125π127π

DISCUSSION

Molecular Electrostatic Potential (MEP).

Figure 6 shows the MEP map of molecules 4, 5 and 19 at 4.5 Å of the nuclei [75].

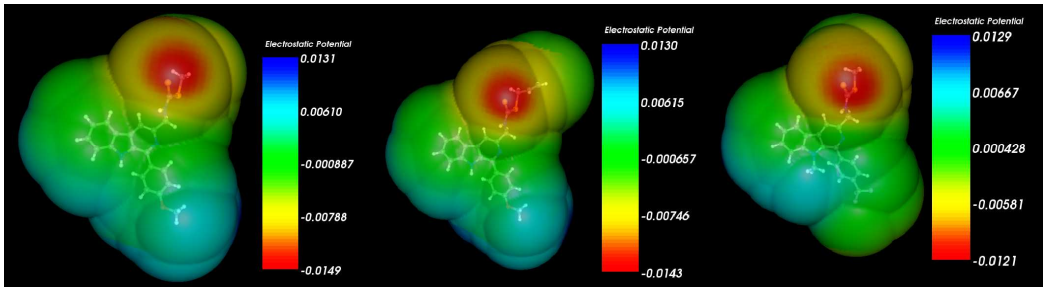

Figure 6. MEP map of molecules 4 (left), 5 (center) and 19 (right) at 4.5 Å of the nuclei

We can observe qualitative similarities in the three maps suggesting that at long molecule-site distances all these molecules can be recognized in a similar way for the binding site. Figure 7 shows the MEP map of molecules 4, 5 and 19 at an $|0.01|$ isovalue [76].

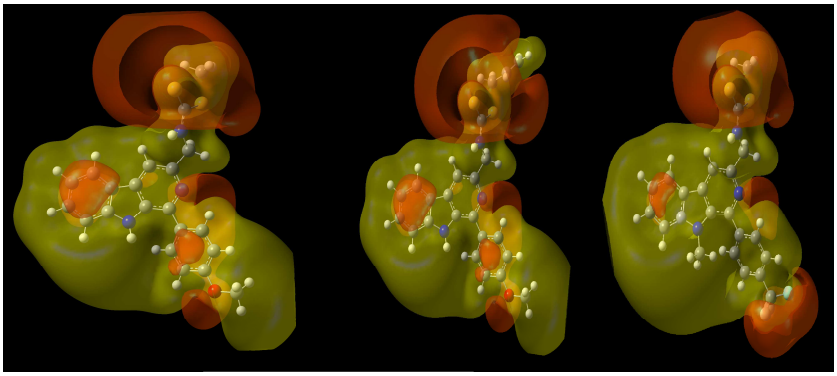

Figure 7. MEP of molecules 4 (left), 5 (center) and 19 (right). The orange isovalue surface corresponds to negative MEP values (-0.01) and the green isovalue surface to positive MEP values (0.01)

We can see that these molecules share similar negative MEP distributions: on ring A, at the *para* substituent of ring D, at N12 in ring D (See Fig. 2) and around the N(S)S fragment. On this basis it is possible to suggest that these molecules interact with the site in an analogous way. We must keep in mind that the conformers displayed in Fig. 7 are not necessarily the one(s) present at the moment of interaction.

Conformational aspects.

The optimized geometries employed here were obtained for calculations carried out *in vacuo*. As an example of conformational freedom, we show in Fig. 8 the superimposition of the lowest energy conformers of molecule 19 (Dreiding Force Field, [77, 78]).

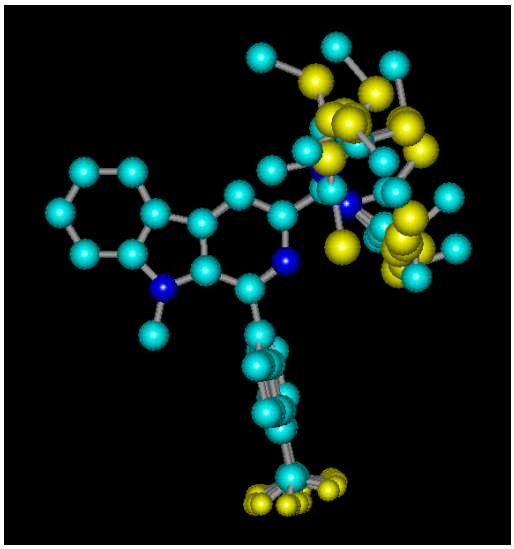

Figure 8. Superimposition of the lowest energy conformers of molecule 19

We can see that this molecule has not a great conformational freedom. This suggests that probably all molecules have a similar conformation at the interaction site involving similar relative positions of rings A, B, D and the N(S)S fragment.

Discussion of cytotoxicity against the A549 cell line

Table 3 shows that the importance of variables in Eq. 1 is $Q_5 >> S_1^N(LUMO+1)* > F_{15}(HOMO-2)* > S_{15}^N(LUMO+1)* > F_{13}(HOMO)* > F_{14}(LUMO+1)*$. A high cytotoxic activity is associated with positive

values for Q_5, high (positive) values for $F_{15}(HOMO-2)*$ and $F_{14}(LUMO+1)*$, and with small (positive) values for $F_{13}(HOMO)*$. The case of the nucleophilic superdelocalizabilities will be discussed below.

Atom 1 is a carbon in ring A (Fig. 2). $(LUMO+1)_1^*$ and $(LUMO)_1^*$ have a π nature (Table 11). If $S_1^N(LUMO+1)*$ is positive, a high cytotoxic activity is associated with a small value for this index. This value is obtained by shifting upwards the associated eigenvalue and making this MO less reactive. Therefore, we suggest that atom 1 is interacting with an electron rich center through its lowest vacant MO. This interaction is probably of π-π kind. Atom 5 is a carbon in ring A (Fig. 2). The positive charge on this atom suggests an electrostatic interaction with a negatively charged moiety. This interaction can be of the cation-π, cation-σ and/or cation-anion. Atom 13 is a carbon in ring C (Fig. 2). $(HOMO)_{13}^*$ has a π nature (Table 12). A high cytotoxic activity is associated with small values for $F_{13}(HOMO)*$. We suggest then that atom 13 is interacting with an electron-rich center. This interaction seems to be of a π-π kind. Atom 14 is a carbon of the CNC(S)S moiety (Fig. 2). $(LUMO+1)_{14}^*$ has a σ nature (Table 12). A high cytotoxic activity is associated with high (positive) values for $F_{14}(LUMO+1)*$. Therefore, it is suggested that atom 14 is interacting with an electron rich center of the binding site. The interactions can be of π-π, π-σ and/or σ-σ kinds. Atom 15 is the nitrogen of the CNC(S)S moiety (Fig. 2). $(HOMO-2)_{15}^*$ has a π nature in almost all molecules, while $(LUMO+1)_{15}^*$ has a π or σ nature (Table 12). A high cytotoxic activity is associated with high values for $F_{15}(HOMO-2)*$. Also, if $S_{15}^N(LUMO+1)*$ is positive, a high cytotoxic activity is associated with a highly reactive $(LUMO+1)_{15}^*$. These two conditions are satisfied if we suggest that atom 15 is interacting simultaneously with an electron rich and an electron-deficient center. The interactions can be of π-π, π-σ and/or σ-σ kinds. All the above suggestions are displayed in the partial 2D pharmacophore of Fig. 9.

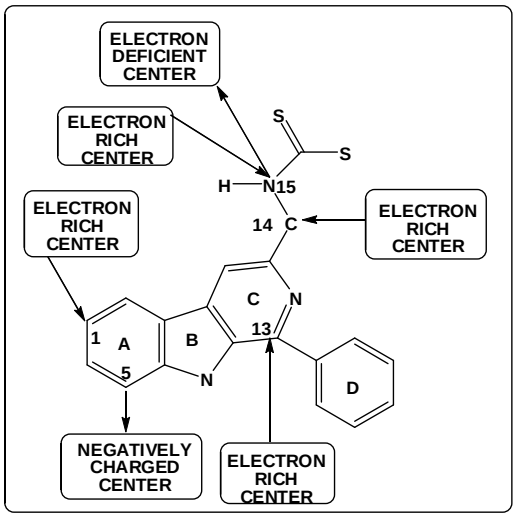

Figure 9. Partial 2D pharmacophore for the cytotoxicity against the A549 cell line

Discussion of cytotoxicity against the mcf-7 cell line.

Table 5 shows that the importance of variables in Eq. 2 is Q_{21}> $F_1(HOMO-1)*$> $S_7^E(HOMO-1)*$= $F_5(LUMO+2)*$>> $S_{12}^E(HOMO-1)*$. A high cytotoxic activity is associated with a positive net charge on atom 21, with a high (positive) numerical value for $F_5(LUMO+2)*$, with a low (positive) numerical value for $F_1(HOMO-1)*$ and with high (negative) values for $S_7^E(HOMO-1)*$ and $S_{12}^E(HOMO-1)*$. Atom 1 is a carbon in ring A (Fig. 2). $(HOMO-1)_1^*$ and $(HOMO-1)_1^*$ have a π nature (Table 11). A low (positive) numerical value for $F_1(HOMO-1)*$ is associated with high cytotoxicity. This suggests that atom 1 is interacting with an electron deficient center through its first highest occupied MO. The interaction is probably of the π-π kind. Atom 5

is a carbon in ring A (Fig. 2). $(LUMO+2)_5^*$, $(LUMO+1)_5^*$ and $(LUMO)_5^*$ have a π nature (Table 11). As a high numerical value for $F_5(LUMO+2)^*$ is associated with high cytotoxicity, we suggest that atom 5 is interacting with an electron rich center. This interaction seems to be of the π-π kind. Atom 7 is a carbon in rings B-C (Fig. 2). $(HOMO-1)_7^*$ and $(HOMO)_7^*$ have a π nature (Table 11). A high negative value for $S_7^E(HOMO-1)^*$ suggests that atom 7 is interacting with an electron deficient center. Again, this interaction seems to be of a π-π kind. Atom 12 is the nitrogen of ring C (Fig. 2). $(HOMO-1)_{12}^*$ may have π or σ natures and $(HOMO-1)_{12}^*$ has a π nature (Table 12). A high negative value for $S_{12}^E(HOMO-1)^*$ suggests that atom 12 is also interacting with an electron deficient center. The interaction(s) can be of π-π, π-σ, σ-π and/or σ-σ kinds. Atom 21 is a carbon in ring D (Fig. 2). A positive net charge, required for high cytotoxicity, suggests that this atom is interacting with a negative moiety located in the binding site. The interaction can be of cation-π, cation-σ and/or anion-cation kinds. All the above suggestions are displayed in the partial 2D pharmacophore of Fig. 10.

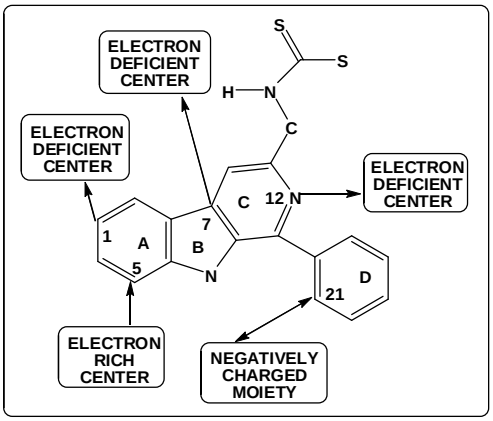

Figure 10. Partial 2D pharmacophore for cytotoxicity against the MCF-7 cell line

Discussion of cytotoxicity against the DU-145 cell line.

Table 7 shows that the importance of variables in Eq. 3 is $F_1(LUMO+1)^* > S_{23}^N(LUMO+1)^* > F_{25}(LUMO+2)^* >> F_{17}(LUMO+2)^* = S_{22}^E(HOMO-1)^* > S_{16}^N(LUMO+2)^*$. A high cytotoxic activity is associated with high (positive) numerical values for $F_{25}(LUMO+2)^*$ and $F_{17}(LUMO+2)^*$, with low (positive) values for $F_1(LUMO+1)^*$ and with high (negative) values for $S_{22}^E(HOMO-1)^*$. The case of the nucleophilic superdelocalizabilities will be discussed below. Atom 1 is a carbon in ring A (Fig. 2). $(LUMO+1)_1^*$ and $(LUMO+1)_1^*$ have a π n nature (Table 11). A high cytotoxicity is associated with low (positive) values for $F_1(LUMO+1)^*$. This suggests that atom 1 is interacting with an electron rich center. It is highly probable that this interaction is of the π-π kind. Atom 16 is a carbon of the CNC(=S)S moiety (Fig. 2). If $S_{16}^N(LUMO+2)^*$ is positive, a high cytotoxicity is associated with high values for this index. This suggests that the three lowest vacant local MOs of this atom are interacting with an electron rich center. $(LUMO)_{16}^*$ has a π nature (Table 13). The nature of $(LUMO)_{16}^*$ and $(LUMO)_{16}^*$ can be π or σ (Table 13). The interactions agreeing with the nature of MOs are of π-π, π-σ, σ-π and/or σ-σ kinds. Atom 17 is a sulphur of the CNC(=S)S moiety (Fig. 2). A high cytotoxic activity is associated with high (positive) numerical values for $F_{17}(LUMO+2)^*$. $(LUMO+2)_{17}^*$, $(LUMO+2)_{17}^*$ and $(LUMO+2)_{17}^*$ have a lone pair nature (Table 13). This suggests that the sulphur atom is interacting with an electron-rich center through its first three lowest vacant MOs, may be through lone pair interactions with a negatively polarized π ring(s). Atom 22 is a carbon in the D ring (Fig. 2). $(HOMO-1)_{22}^*$ and $(HOMO-1)_{22}^*$ have π or σ natures (Table 13). Note that $(HOMO)_{22}^*$ and $(LUMO)_{22}^*$ are very far from the corresponding frontier MOs. A high cytotoxic activity is associated with high (negative) values for $S_{22}^E(HOMO-1)^*$. This suggests that atom 22 is interacting with an electron deficient center. Possible interactions are of π-π, π-σ, σ-π and/or σ-σ types. Atom 23 is a

carbon in the D ring (Fig. 2). $(LUMO)_{23}^{*}$ and $(LUMO+1)_{23}^{*}$ have σ or π natures (Table 14). In this case $(HOMO)_{23}^{*}$ and $(LUMO)_{23}^{*}$ are very far from the corresponding frontier MOs. If $S_{23}^{N}(LUMO+1)*$ is positive, a high cytotoxic activity is associated with small values for this index, making the corresponding MO less reactive. For this reasons we suggest that atom 23 is interacting with an electron rich center through its first vacant local MO. Possible interactions are of π-π, π-σ, σ-π and/or σ-σ kinds. Atom 25 is a carbon in ring D (Fig. 2). $(LUMO)_{25}^{*}$, $(LUMO+1)_{25}^{*}$ and $(LUMO+2)_{25}^{*}$ have π or σ natures (Table 14). A high cytotoxicity is associated with high (positive) numerical values for $F_{25}(LUMO+2)*$. Therefore, we suggest that atom 25 is interacting with an electron-rich center. The interactions can be of the π-π, π-σ, σ-π and/or σ-σ types. All the suggestions are displayed in the partial 2D pharmacophore of Fig. 11.

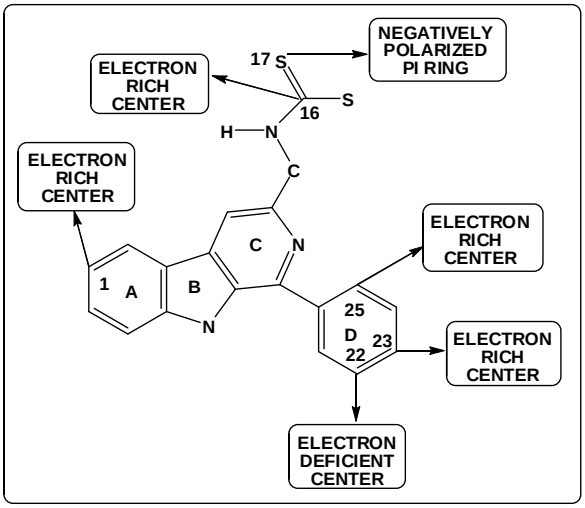

Figure 11. Partial 2D pharmacophore for cytotoxicity against the DU-145 cell line

Discussion of cytotoxicity against the HeLa cell line.

Table 9 shows that the importance of variables in Eq. 4 is $S_6^E(HOMO-1)*$>> $S_{17}^N(LUMO+1)*$> $F_{15}(LUMO+1)*$> $S_{22}^E(HOMO-1)*$> $F_{12}(LUMO+2)*$. A high cytotoxic activity is associated with high (positive) numerical values for $F_{15}(LUMO+1)*$ and $F_{12}(LUMO+2)*$, with small (negative) values for $S_6^E(HOMO-1)*$ and with high (negative) values for $S_{22}^E(HOMO-1)*$. $S_{17}^N(LUMO+1)*$ will be discussed below. Atom 6 is a carbon in ring A (Fig. 2). $(HOMO-1)_6^{*}$ and $(HOMO)_6^{*}$ have a π nature (Table 16). A high cytotoxicity is associated with small (negative) values for $S_6^E(HOMO-1)*$. This suggests that atom 6 is interacting, through its highest occupied local MO, with an electron-deficient moiety. The interaction is possible of a π-π kind. Atom 12 is the nitrogen in ring C (Fig. 2). $(LUMO)_{12}^{*}$, $(LUMO+1)_{12}^{*}$ and $(LUMO+2)_{12}^{*}$ have a π nature (Table 12). A high cytotoxicity is associated with high (positive) values for $F_{12}(LUMO+2)*$. We suggest that atom 12 is interacting with an electron rich center through its first three lowest vacant MOs. The interaction is possible of a π-π kind. Atom 15 is the nitrogen in the CNC(=S)S moiety (Fig. 2). $(LUMO)_{15}^{*}$ and $(LUMO)_{15}^{*}$ have π or σ natures (Table 12). A high cytotoxic activity is associated with high (positive) numerical values for $F_{15}(LUMO+1)*$. For this reasons we suggest that atom 15 is interacting with an electron rich center through its first two vacant local MOs. Possible interactions are of π-π, π-σ, σ-π and/or σ-σ kinds. Atom 17 is the sulphur in the CNC(=S)S moiety (Fig. 2). $(LUMO)_{17}^{*}$ and $(LUMO+1)_{17}^{*}$ have a lone pair nature (Table 13). If $S_{17}^{N}(LUMO+1)*$ is positive, a high cytotoxicity is associated with high values for this index. This suggests that this atom is interacting with an electron-rich center through its first two lowest vacant MOs, possibly through lone pair interactions with a negatively polarized π ring(s). Atom 22 is a carbon in ring D (Fig. 2). $(HOMO)_{22}^{*}$ and $(HOMO-1)_{22}^{*}$ have π or σ natures (Table 13). These local MOs are very far from the corresponding molecular

frontier MOs. A high cytotoxicity is associated with high (negative) values for $S_{22}^{E}(HOMO-1)^{*}$. This suggests that this atom is interacting with an electron deficient center. Possible interactions are of π-π, π-σ, σ-π and/or σ-σ kinds. All the suggestions are displayed in the partial 2D pharmacophore of Fig. 12.

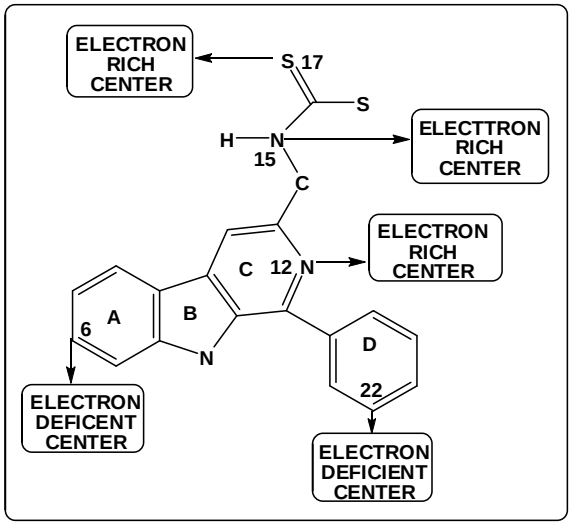

Figure 12. Partial 2D pharmacophore for cytotoxicity against the HeLa cell line

In summary, we have obtained statistically significant relationships between the electronic structure and the cytotoxicity against four cancer cell lines for a series of β-carboline-dithiocarbamate derivatives. The corresponding pharmacophores have been built. Our results provide information serving for a better understanding of this biological process.

REFERENCES

[1] H-z Xuan, J-h Zhang, Y-h Wang, C-l Fu, W Zhang, *Bioorg. Med. Chem. Lett.*, **2016**, 26, 570-574.
[2] J Wu, C Yang, C Guo, X Li, N Yang, et al., *Chem.-Biol. Int.*, **2016**, 244, 94-104.
[3] L Venables, TC Koekemoer, M Van de Venter, ED Goosen, *South Af. J. Bot.*, **2016**, 103, 216-221.
[4] J Mancini, P Rousseau, KJ Castor, HF Sleiman, C Autexier, *Biochim.*, **2016**, 121, 287-297.
[5] V Jamsheena, G Shilpa, J Saranya, NA Harry, RS Lankalapalli, et al., *Chem.-Biol. Int.*, **2016**, 247, 11-21.
[6] Z Gagic, K Nikolic, B Ivkovic, S Filipic, D Agbaba, *J. Taiwan Inst. Chem. Engn.*, **2016**, 59, 33-44.
[7] T E-kobon, P Thongararm, S Roytrakul, L Meesuk, P Chumnanpuen, *Comp. Struct. Biotech. J.*, **2016**, 14, 49-57.
[8] EP Carreiro, AR Costa, MM Cordeiro, R Martins, TO Pires, et al., *Bioorg. Med. Chem. Lett.*, **2016**, 26, 1039-1043.
[9] M Zhou, S Ji, Z Wu, Y Li, W Zheng, et al., *Eur. J. Med. Chem.*, **2015**, 96, 92-97.
[10] A Zajdel, A Wilczok, M Tarkowski, *Toxicol. In Vitro*, **2015**, 30, 486-491.
[11] NI Sulaiman, NR Salimin, RA Haque, MA Iqbal, SW Ng, et al., *Polyhedron*, **2015**, 97, 188-196.
[12] L Soliño, FX Sureda, J Diogène, *Toxicol. In Vitro*, **2015**, 29, 59-62.
[13] J-h Shao, G-h Feng, *Chin. Med. Sci. J.*, **2015**, 30, 260-265.
[14] P Ramadevi, R Singh, SS Jana, R Devkar, D Chakraborty, *J. Photochem. Photobiol. A.*, **2015**, 305, 1-10.
[15] JYH Ong, PVC Yong, YM Lim, ASH Ho, *Life Sci.*, **2015**, 135, 158-164.
[16] T Marudhupandi, TT Ajith Kumar, S Lakshmanasenthil, G Suja, T Vinothkumar, *Int. J. Biol. Macromol.*, **2015**, 72, 919-923.
[17] M Lei, X Gan, K Zhao, Q Yu, L Hu, *Bioorg. Med. Chem. Lett.*, **2015**, 25, 435-437.
[18] RM Kumbhare, TL Dadmal, MJ Ramaiah, KSV Kishore, SNCVL Pushpa Valli, et al., *Bioorg. Med. Chem. Lett.*, **2015**, 25, 654-658.
[19] T-y Gao, X Jin, W-z Tang, X-j Wang, Y-x Zhao, *Bioorg. Med. Chem. Lett.*, **2015**, 25, 3686-3689.
[20] D Dimić, AG Mercader, EA Castro, *Chemom. Int. Lab. Sys.*, **2015**, 146, 378-384.
[21] S Cho, MJ Choi, M Kim, S Lee, J Lee, et al., *J. Mol. Struct.*, **2015**, 1084, 294-301.

[22] MK Zilla, D Nayak, H Amin, Y Nalli, B Rah, et al., *Chem.-Biol. Int.*, **2014**, 224, 100-107.
[23] X-W Zhou, H-L Ma, X Zhang, S-Y Jing, J-Y Miao, et al., *Eur. J. Med. Chem.*, **2014**, 79, 95-101.
[24] J-F Zhang, M Li, J-Y Miao, B-X Zhao, *Eur. J. Med. Chem.*, **2014**, 83, 516-525.
[25] R Talaat, W El-Sayed, H Agwa, A Gamal-Eldeen, S Moawia, et al., *Biomed. Ag. Pathol.*, **2014**, 4, 179-189.
[26] K Masawang, M Pedro, H Cidade, RM Reis, MP Neves, et al., *Toxicol. Lett.*, **2014**, 229, 393-401.
[27] J Kim, GK Jayaprakasha, BS Patil, *Biochim.*, **2014**, 105, 36-44.
[28] D-J Chen, H-M Liu, S-F Xing, X-L Piao, *Bioorg. Med. Chem. Lett.*, **2014**, 24, 186-191.
[29] AH Banday, AK Giri, R Parveen, N Bashir, *Steroids*, **2014**, 87, 93-98.
[30] Note. The results presented here are obtained from what is now a routinary procedure. For this reason, we built a general model for the paper's structure. This model contains *standard* phrases for the presentation of the methods, calculations and results because they do not need to be rewritten repeatedly.
[31] JS Gómez-Jeria, *Canad. Chem. Trans.*, **2013**, 1, 25-55.
[32] JS Gómez-Jeria, *Elements of Molecular Electronic Pharmacology (in Spanish)*, Ediciones Sokar, Santiago de Chile, **2013**.
[33] T Bruna-Larenas, JS Gómez-Jeria, *Int. J. Med. Chem.*, **2012**, 2012 Article ID 682495, 1-16.
[34] JS Gómez-Jeria, M Ojeda-Vergara, *J. Chil. Chem. Soc.*, **2003**, 48, 119-124.
[35] JS Gómez-Jeria, "Modeling the Drug-Receptor Interaction in Quantum Pharmacology," in *Molecules in Physics, Chemistry, and Biology*, J. Maruani Ed., vol. 4, pp. 215-231, Springer Netherlands, **1989**.
[36] JS Gómez-Jeria, *Int. J. Quant. Chem.*, **1983**, 23, 1969-1972.
[37] F Peradejordi, AN Martin, A Cammarata, *J. Pharm. Sci.*, **1971**, 60, 576-582.
[38] JS Gómez-Jeria, *Res. J. Pharmac. Biol. Chem. Sci.*, **2016**, in press,
[39] JS Gómez-Jeria, M Ojeda-Vergara, C Donoso-Espinoza, *Mol. Engn.*, **1995**, 5, 391-401.
[40] MS Leal, A Robles-Navarro, JS Gómez-Jeria, *Der Pharm. Lett.*, **2015**, 7, 54-66.
[41] JS Gómez-Jeria, J Valdebenito-Gamboa, *Res. J. Pharmac. Biol. Chem. Sci.*, **2015**, 6, 203-218.
[42] JS Gómez-Jeria, J Valdebenito-Gamboa, *Der Pharma Chem.*, **2015**, 7, 323-347.
[43] JS Gómez-Jeria, A Robles-Navarro, *Res. J. Pharmac. Biol. Chem. Sci.*, **2015**, 6, 1358-1373.
[44] JS Gómez-Jeria, A Robles-Navarro, *Res. J. Pharmac. Biol. Chem. Sci.*, **2015**, 6, 1811-1841.
[45] JS Gómez-Jeria, A Robles-Navarro, *J. Comput. Methods Drug Des.*, **2015**, 5, 15-26.
[46] JS Gómez-Jeria, *J. Chil. Chem. Soc.*, **2010**, 55, 381-384.
[47] JS Gómez-Jeria, F Soto-Morales, J Rivas, A Sotomayor, *J. Chil. Chem. Soc.*, **2008**, 53, 1393-1399.
[48] JS Gómez-Jeria, LA Gerli-Candia, SM Hurtado, *J. Chil. Chem. Soc.*, **2004**, 49, 307-312.
[49] JS Gómez-Jeria, F Soto-Morales, G Larenas-Gutierrez, *Ir. Int. J. Sci.*, **2003**, 4, 151-164.
[50] JS Gómez-Jeria, L Lagos-Arancibia, *Int. J. Quant. Chem.*, **1999**, 71, 505-511.
[51] JS Gómez-Jeria, D Morales-Lagos, JI Rodriguez-Gatica, JC Saavedra-Aguilar, *Int. J. Quant. Chem.*, **1985**, 28, 421-428.
[52] JS Gómez-Jeria, DR Morales-Lagos, *J. Pharm. Sci.*, **1984**, 73, 1725-1728.
[53] JS Gómez-Jeria, D Morales-Lagos, "The mode of binding of phenylalkylamines to the Serotonergic Receptor," in *QSAR in design of Bioactive Drugs*, M. Kuchar Ed., pp. 145-173, Prous, J.R., Barcelona, Spain, **1984**.
[54] A Robles-Navarro, JS Gómez-Jeria, *Der Pharma Chem.*, **2016**, 8, 417-440.
[55] JS Gómez-Jeria, C Moreno-Rojas, *Der Pharma Chem.*, **2016**, 8, 475-482.
[56] JS Gómez-Jeria, J Valdebenito-Gamboa, *Der Pharma Chem.*, **2015**, 7, 103-121.
[57] JS Gómez-Jeria, A Robles-Navarro, *Res. J. Pharmac. Biol. Chem. Sci.*, **2015**, 6, 755-783.
[58] JS Gómez-Jeria, A Robles-Navarro, *Res. J. Pharmac. Biol. Chem. Sci.*, **2015**, 6, 1337-1351.
[59] JS Gómez-Jeria, MB Becerra-Ruiz, *Der Pharma Chem.*, **2015**, 7, 362-369.
[60] DI Pino-Ramírez, JS Gómez-Jeria, *Amer. Chem. Sci. J.*, **2014**, 4, 554-575.
[61] D Muñoz-Gacitúa, JS Gómez-Jeria, *J. Comput. Methods Drug Des.*, **2014**, 4, 48-63.
[62] D Muñoz-Gacitúa, JS Gómez-Jeria, *J. Comput. Methods Drug Des.*, **2014**, 4, 33-47.
[63] JS Gómez-Jeria, *Res. J. Pharmac. Biol. Chem. Sci.*, **2014**, 5, 780-792.
[64] JS Gómez-Jeria, *J. Comput. Methods Drug Des.*, **2014**, 4, 32-44.
[65] JS Gómez-Jeria, *Der Pharma Chem.*, **2014**, 6, 64-77.
[66] I Reyes-Díaz, JS Gómez-Jeria, *J. Comput. Methods Drug Des.*, **2013**, 3, 11-21.
[67] A Paz de la Vega, DA Alarcón, JS Gómez-Jeria, *J. Chil. Chem. Soc.*, **2013**, 58, 1842-1851.
[68] JS Gómez-Jeria, M Flores-Catalán, *Canad. Chem. Trans.*, **2013**, 1, 215-237.
[69] C Barahona-Urbina, S Nuñez-Gonzalez, JS Gómez-Jeria, *J. Chil. Chem. Soc.*, **2012**, 57, 1497-1503.
[70] A Kamal, M Sathish, VL Nayak, V Srinivasulu, B Kavitha, et al., *Bioorg. Med. Chem.*, **2015**, 23, 5511-5526.

[71] MJ Frisch, GW Trucks, HB Schlegel, GE Scuseria, MA Robb, et al., "G03 Rev. E.01," Gaussian, Pittsburgh, PA, USA, **2007**.
[72] JS Gómez-Jeria, "D-Cent-QSAR: A program to generate Local Atomic Reactivity Indices from Gaussian 03 log files. v. 1.0," Santiago, Chile, **2014**.
[73] JS Gómez-Jeria, *J. Chil. Chem. Soc.*, **2009**, 54, 482-485.
[74] Statsoft, "Statistica v. 8.0," 2300 East 14 th St. Tulsa, OK 74104, USA, **1984**-**2007**.
[75] M Hanwell, D Curtis, D Lonie, T Vandermeersch, E Zurek, et al., *Journal of Cheminformatics*, **2012**, 4, 17.
[76] RD Dennington, TA Keith, JM Millam, "GaussViev 5.0.8," GaussViev 5.0.8, 340 Quinnipiac St., Bldg. 40, Wallingford, CT 06492, USA, **2000**-**2008**.
[77] Hypercube, "Hyperchem 7.01," 419 Phillip St., Waterloo, Ontario, Canada, **2002**.
[78] Chemaxon, "MarvinView," www.chemaxon.com, USA, **2014**.